Scientific Journal for faculty of Science - Sirte University

ISSN: 2789-858X

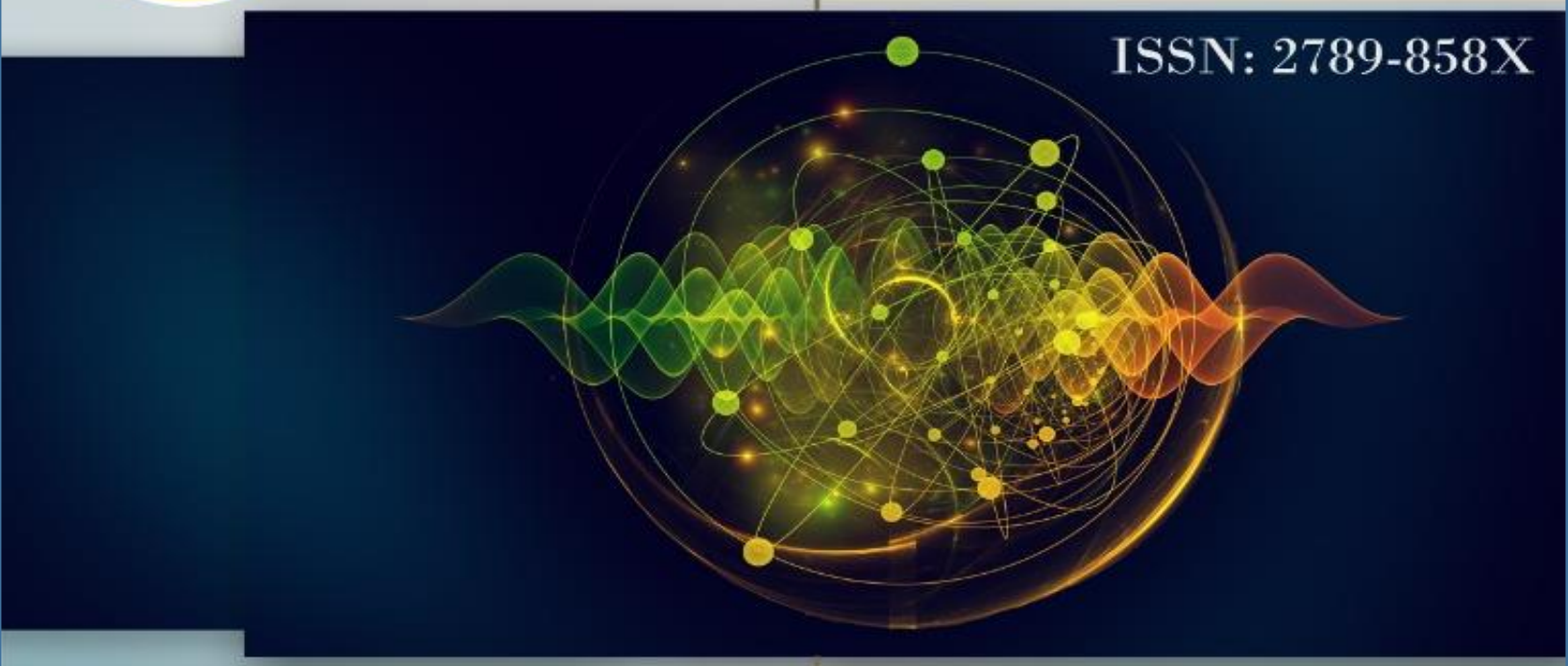

Volume1 Issue No.2 October 2021

Bi-annual Peer-review Journal

Legal Deposit Number: 990/2021

sjsfsu@su.edu.ly
journal.su.edu.ly/index.php/JSFSU

Scientific Journal for the Faculty of Science-Sirte University Vol 1, No 2, October (2021) 41-51

Scientific Journal for the Faculty of Science-Sirte University (SJFSSU)

Journal home page: http://journal.su.edu.ly/index.php/JSFSU/index

Design and Simulation of a Piezoresistive V-Shaped Strain Gauge for Torque Measring

M. Hilal Muftah[1], K . Petroczki[2], E. Awad Khidir[3] and A. A. Borhana[4]

[1] *Computer Science Department, Science Faculty, Sirte University, 674 Sirte, Libya. .*
[2]*Department of Agra-energetics and foods Engineering, Faculty of Mechanical Engineering, Szent Istvan University, H 2103, Godollo, Hungary*
[3] *Mechanical and Material Engineering Department, Engineering and the Built Environment Faculty, Universiti Kebangsaan Malaysia, 43600 UKM Bangi, Malaysia*
[4]*Mechanical Engineering Department, Engineering College, Universiti Tenaga Nasional, Putrajaya Campus, Jalan IKRAM-UNITEN, 43000 Kajang, Selangor, Malaysia.*

ARTICLE INFO

Article history:
Received 9 August 2021
Received in revised form 21October 2021
Accepted 22 October 2021

Keywords:
Finite Element Analysis,
Metal Strain Gauge,
Rotating Shaft,
Torque,
Computer software ANSYS.

ABSTRACT

Modeling and simulation of system design adjustment is respectable training for design and engineering decisions in real world jobs. In this paper, the exact perseverance connected with the strain of components is very important for structural designs, analyses, and for excellent control. The information linked to this type of test is usually related to the exact dimensions connected with the pressure within a flexible region. This paper proposed the design and simulation of a torque sensor with a piezoresistive V-shaped strain gauge. The piezoresistive measure of a precious metal for a stable base was made according to the results of an ANSYS simulation. A torque sensor with a piezoresistive V-shaped tension measure on a base was made. The result of the particular simulation shifted the fraction of tension on the base to enable the torque on the substrate to be measured. Theoretical studies on the piezoresistive measure of a metal for the stable base as well as the torque sensor were introduced. A maximum of 127.29 με and a maximum resistance change in gauge equal to 0.091Ω were achieved for an applied torque of 22.0725 Nm. Here, computer systems modeling and simulation are going to be used.

1 Introduction

Certain types of tension causes torque, which results in an alteration in the level of resistance, which can then be tested. The detailed process involving the measurement of the resistivity of a material is based on the belief that any power conductor uses kinetic energy to change the level of resistance. This is because micro structural changes within the conductor occur across the parts and affect the resistivity. The size of the strain is often determined by the exposed area or maybe through the topography of the subject under tension. There is no physical control in the selection of the gauge measurements (Joyce & Scott, 1993). The strain gauge calculations are based on the minor refraction principle (Eaton et al., 1999; Szilard, 1974). A specific simulation application, ANSYS, is needed to find the maximum stress indication area within the whole length. The idea enables the specified alignment to be determined in addition to the active

Corresponding author:
E-mail: muftah19@su.edu.ly
DOI: https://doi.org/10.37375/sjfssu.v1i2.70

area within the whole length to attain the maximum tenderness. Materials such as aluminium, polystyrene, silicon, and polyimide are utilized as substrates for the design of the strain gauge (Hamid et al., 2006;Thangamani et al., 2008; Yang & Lu, 2013). Lightweight aluminium is capable of exerting the greatest strain and is suitable for use within a temperature range of -195 ˚C to +400 ˚C, and therefore, in this particular study, it was selected as a substrate for the pattern assessment. Lightweight aluminium is usually an ideal substrate for general objective static as well as active pressure evaluations. An isoelastic combination was used for the assessment of the strain pattern (grid) of a popular piezoresistive steel product. Due to the large peel power of the material, it was possible to actually assess a smaller amount of it due to mechanical damage during installation (Schomburg et al., 2004; Window & Holister, 1982). Concerning the data for these studies, no theoretical research is available so far on the strain measurement of piezoresistive metallic gauges on a solid shaft. In current researches, equations are usually produced regarding the strain measurement of piezoresistive metallic gauges within a comprehensive base. The strain supplied by any torque sensor using this strain gauge and its individual components was analysed. Furthermore, the measurement of the strain that was converted from one part to another was taken into consideration. This feature was exploited to successfully select the precise material for the design. Several disk for torque measuring sensors technologically advanced into spoke-type assemblies, as an alternative, depiction strain on the at right angles or cross spoke-surface with a twisting distortion approach (Wang Y.J. et al, 2017; Hu G.Y et al,2018; Li X. et al, 2019). A Lever-Type Method of Strain Exposure for Disk F-Shaped Torque Sensor Design reported by (Ran Shu et al., 2020). This paper presents a lever-type method of strain exposure that performs a uniaxial tension and compression deformation mode to optimize the strain uniformity and improve the trade-off. Moreover, on the basis of this approach, the proposed disk F-shaped torque sensor enjoys has axial thinness, easy installation of strain gauges and flexible customization. The simulation and experimental results have validated the basic design idea

2 Material for the strain gauge

In this paper, a piezoresistive isoelastic material was chosen for the strain gauge design due to its high sensitivity, as shown in Table 1. It has been used for the commercial production of strain gauges as it also has high fatigue strength, which enables the strain gauges to be used normally in the case of harmonic loads with strain values not exceeding 1500με. However, due to its sensitivity to temperature, it was necessary to use a Wheatstone bridge.

. Table 1 Gauge factors using different materials (J.W. Dally & W.F. Riley, 1991)

Material	Percentage %	K (Sensitivity)
Advance (Constantan)	45 Ni, 55 Cu	2.1
Nichrome V	80 Ni, 20 Cr	2.1
Isoelastic	36 Ni, 8 Cr, 0.5 Mo, 55.5 Fe	3.6
Karma	74 Ni, 20 Cr, 3 Al, 3 Fe	2.0
Armour D	70 Fe, 20 Cr, 10Al	2.0
Platinum-Tungsten (479)	92 Pt, 8 W	4.1

2.1 Substrate Material

There are many materials, in fact, that can be used for the substrate without affecting the operation of devices. In this study, aluminium was selected as the substrate material for the strain gauge because it is a common material that is cheap and can be easily glued with epoxy or cyanoacrylate as shown in the Figure

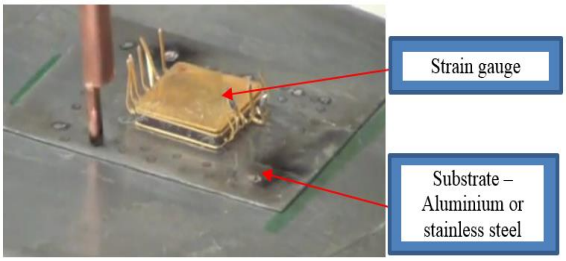

Fig. 1 welding strain gauge to substrate

Welding strain gauge to substrate, a special type of glue is used to attach strain gauges to the substrate. The type of glue depends on the required lifetime of the measurement system. For short-term measurements (up to a few weeks), cyanoacrylate glue is appropriate, while for long lasting installations, epoxy glue is required. Usually, epoxy glue requires curing at a high temperature (about 80-100 °C). The preparation of the surface where the strain gauge is to be glued is of the utmost importance.

The surface must be smoothed (e.g. with very fine sandpaper) and de-oiled with solvents. Traces of the solvents must then be removed and the strain gauge must be glued immediately after this to avoid oxidation or pollution of the prepared area. If these steps are not followed, the binding of the strain gauge to the surface may be unreliable, and unpredictable measurement errors may be generated. Strain gauge-based technology is commonly utilized in the manufacture of pressure sensors. The gauges used in pressure sensors are usually made of silicon, polysilicon, metal films, thick films, and bonded foils.

2.2 Theoretical Study

The adjustment in the strain gauge resistance on the shaft caused by an applied torque was determined by the strain that was exerted on the shaft and transferred to the gauge. This will be investigated in the following sections.

2.3 Strain on the Solid Shaft

The equation (1) is used to determine the effective torsion moment, M_t from which the transferred power, P can be computed for a rotating shaft in order to calculate the strain for a full bridge:

$$\varepsilon_i = \frac{2\,M_t}{G \cdot S_p} \qquad (1)$$

The shear modulus, G renders the shear stress calculations less complex as it identifies an independent material parameter such as Young's modulus, E = 202 kN/mm2 and Poisson's ratio, v = 0.28, and can then be derived from these (Hoffmann, 1989; Young & Budynas, 2002).

$$G = \frac{E}{2(1+v)} \qquad (2)$$

In the case of a cylindrical shaft with diameter of 28 mm, the polar section modulus of the shaft as follows:

$$S_p = \frac{\pi \cdot d^3}{16} \approx 0.2d^3 \qquad (3)$$

Formerly, maximum strain was calculated through the utilization of 127.29 με (1.2729E-04), for a full bridge circuit (4SGs) at torque, M_t = 22.0725Nm. The bridge factor then was equal to 4, and the strain for each resistance was equal to 31.82με (31.81E-06).

Table 2 Strain in the Shaft

Case	Torque (Nm)	Strain in Shaft (%)
1	0.0000	0.0000
2	2.4525	1.4143E-05
3	4.9050	2.8286E-05
4	7.3575	4.2430E-05
5	9.8100	5.6573E-05
6	12.2625	7.0716E-05
7	14.7150	8.4859E-05
8	17.1675	9.9002E-05
9	19.6200	1.1315E-04
10	22.0725	1.2729E-04

2.4 Strain on the Gauge

Strain is measured by changes in the electrical resistance of a sensor known as a strain gauge. This is mainly based on the fact that when a material is strained, the metallic material resistance is increased (Micro-Measurements, 2007; Murray & Miller, 1992). The resistance (*R*) of the gauge can be determined as follows:

$$R = \rho \frac{L}{A} \qquad (4)$$

where:

L: the length of the material,

A: the area, and

ρ: the specific resistance.

According to the above expression, the resistor length is related to the resistance, and any variation in the resistance will be displayed by a variation in the length. Strain is measured by the strain gauge based on changes in the acceptable mechanical variation of electrical signals. A strain gauge null point varies according to the temperature variation, and this is

called the measuring error. A Wheatstone bridge is generally used for increasing the signal or for the calibration of the temperature variation results, hence making available a more precise measurement (Eberlein, 2008). Four resistors were used in the design of the Wheatstone bridge, as shown in Figure 2. There are three types of Wheatstone bridge constructions, namely a Full Bridge, Half Bridge, and lastly, a Quarter Bridge, where a single resistance is recycled in the Wheatstone bridge (Micro-Measurements, 2007).

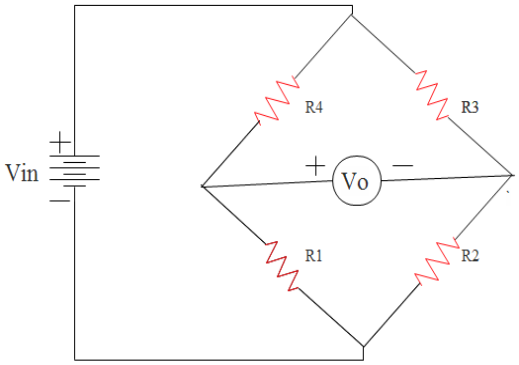

Fig. 2 Wheatstone bridge

The drop in the voltage for both the resistances, R_1 and R_4, was obtained using the following diagram and equations:

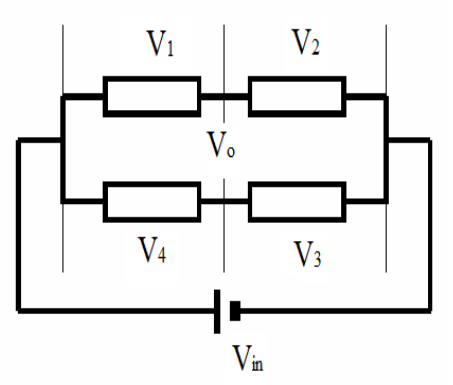

Fig. 3 Applying the Wheatstone bridge circuit

$$V_{o\,R_1} = \frac{R_1}{R_1+R_2} V_{in} \quad (5)$$

$$V_{o\,R_4} = \frac{R_4}{R_3+R_4} V_{in} \quad (6)$$

$$V_o = V_{o\,R_1} - V_{o\,R_4} = \frac{R_1}{R_1+R_2} V_{in} - \frac{R_4}{R_3+R_4} V_{in} \quad (7)$$

$$V_o = V_{in}\left(\frac{R_1+\Delta R_1}{R_1+\Delta R_1+R_2+\Delta R_2} - \frac{R_4+\Delta R_4}{R_3+\Delta R_3+R_4+\Delta R_4}\right) \quad (8)$$

The changes in the resistances in the strain gauges were too slight: $\Delta R \ll R$

Each half of the Wheatstone bridge had a similar resistance: $R_1 = R_2$ and $R_3 = R_4$

$$\frac{V_o}{V_{in}} = \frac{\Delta R_1}{R_1} - \frac{\Delta R_2}{R_2} + \frac{\Delta R_3}{R_3} - \frac{\Delta R_4}{\Delta R_4} \quad (9)$$

By means of:

$$\frac{\Delta R}{R} = K\varepsilon \quad (10)$$

it was implied that:

$$\frac{V_o}{V_{in}} = \frac{K}{4}(\varepsilon_1 - \varepsilon_2 + \varepsilon_3 - \varepsilon_4) \quad (11)$$

In the case of the measurements on a shaft under torsion (Full Bridge), the changes in the resistance of the strain gauge were calculated using Equation (10), while the changes in the gauge voltage were obtained using Equation (11). For the measurements on a shaft under rotation (Full Bridge) and with temperature compensations, strain gauge 1 and strain gauge 3 were positive, while strain gauge 2 and strain gauge 4 were negative (Eberlein, 2008). However, when applied to the standard and compensated bending strains, strain gauge 1 and strain gauge 4 were positive, while strain gauge 2 and strain gauge 3 were negative (Eberlein, 2008). The Wheatstone Bridge Circuit was used at every stage using four resistors. These four resistors may possibly be with only one, two or four strain gauges. If four active strain gauges are used, the largest output value will be obtained. Moreover, modern amplifiers are used in place of "missing" resistors in the Wheatstone Bridge Circuit (Eberlein, 2008; Micro-Measurements, 2007).

2.5 Torque Measurement

The particular piezoresistive V-shaped strain gauge designed by ANSYS was the result of a simulation employed to develop a torque sensor. To create the torque sensor, any risk from the strain gauge was actually pre-set. The further development of the Wheatstone bridge with a V-shaped strain gauge is shown in Figure 4. The next figure exhibits the testing

of the torque by means of tension gauges. The particular torque was tested using the tension sensor with a diameter (d) of 28 mm. In this case, the sensor actually rubber stamped some lively links that had been determined and proven, as shown in Figure 3 below (Korzenszky 2009).

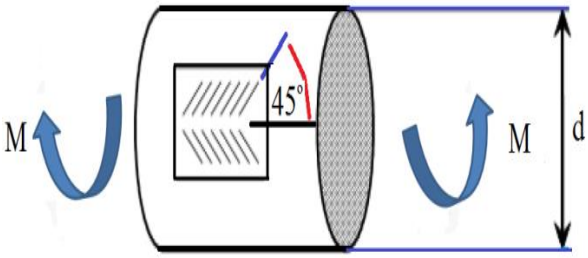

Fig. 4 Twisted shaft diameter, d and "Fishbone" stamp (Korzenszky, 2009)

3 Simulation

The particular finite element analysis computer software ANSYS was used to obtain the strain that was supplied and the strain that was working on the sensor parts (Cao et al., 2000; Lin et al.,1999; Orhan et al., 2001). The CATIA software design tool was utilized to design the sensor modules such as the shaft, substrate and the strain gauge. The dimensions of the strain gauge and the parts of the torsional shaft were employed for the geometrical analysis. The dimensions were utilized to modify all the tools in the CATIA software and to export them to the STEP file. Moreover, the STEP file created by the CATIA software and the mesh model were imported for the simulation process. Then, the data to the Steady-State module was transferred to the simulation workbench.

As revealed in Figure 4, it was necessary to detect any risk of strain submission in order to find the utmost strained location within the base to determine the design. This permitted the development of a hypersensitive strain gauge. On the other hand, the load computations of the sensor parts were employed to compute the percentage of the strain that was transmitted from one section to other parts. This helped to reveal the utmost strained parts, and most of these strains, as shown in Tables 4 and 5.

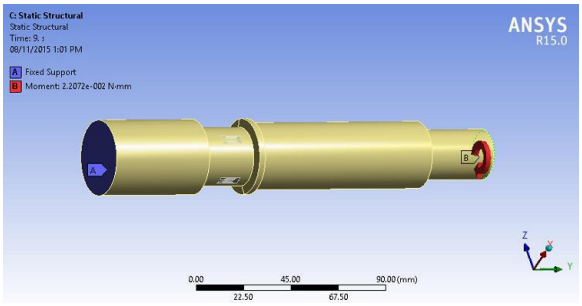

Fig. 5 Location of strain gauge and load, and boundary conditions

4 Strain Gauge

In this paper, a novel strain gauge was simulated for the preferred torque measurements. The space for the determined strained area, i.e., the active area for the gauge plan, was set at 3.76 mm x 2.678 mm, as shown in Figure 6. Moreover, a substrate with a length of 20 mm, width of 9 mm, and thickness of 0.5 mm was preferred in this study for the project and examination.

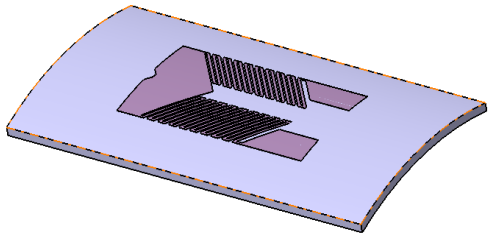

Fig. 6 Configuration of torsional strain gauge model

The simulation of the clamped and supported edge boundary conditions was performed on the substrate. The maximum and minimum strains that were created in the strained areas of both the clamped and supported edge substrates were calculated. At the stretched side edges, the maximum strain placed on the supported edges was found. Subsequently, the minimum strained places were also determined and were found to be at the centre. Hence, the position of the gauge in the centre region was insensitive. Therefore, the clamped edge boundary condition was utilized in the design of the strain gauge. The substrate mesh element matrix had a partition size of 200 x 90 element matrices since the dimensions were 20 mm x 9 mm. As a result of the control at the junction, the mesh division matrix dimensions should not exceed 200 x 90 element matrices. Although an increase in the matrix partition led to an increase in the strain, the maximum increase in strain was moved closer to the stretched side limits.

For smaller matrix sizes, the distribution area of the maximum strain stayed at the centre, while the strain rate of that area decreased. As a result, the maximum strain rate and its equivalent strain range were established on the junction boundaries.

An 8-loop strain gauge was considered in this study since a similar number of loop gauges are used in the manufactured product. The gauge (grid) pattern was planned and constructed on the determined strain part for an active length of 2.678 mm, with single line widths of 0.4 mm and 0.07 mm, and a thickness of 0.005 mm. The shaft and the gauge were meshed individually while maintaining the stability. Then, the determined strain (shown in black) was focused at the centre and the areas near the shaft, which had a diameter of 28 mm. The piezoresistive gauge was then arranged within this area.

In order to simulate a problem, it was necessary to create the geometry and to perform the meshing before using the ANSYS Meshing to process and solve the problem. The geometry can be created by using CAD software such as ANSYS GEOMETRY, CATIA, SOLIDWORK, etc., while meshing can be carried out by using ANSYS meshing, ICEM CFD, HYPERMESH, etc. Meshing is an important step in FEA as it affects the convergence process. The piezoresistive math model requires a fine mesh for more accurate results. Additionally, the powerful ANSYS Meshing tool was used to manage the size and shape of the mesh. The mesh and time steps are inherent parts of the model. Strain gauge models make use of the grid scale. If the mesh resolution is anisotropic, for example, the longer length scale may also have an unnecessarily negative effect. For this reason, the use of isotropic grids should be considered, perhaps replacing the use of hexahedral elements with tetrahedral ones. Figure 7 shows the elements and the meshing shape.

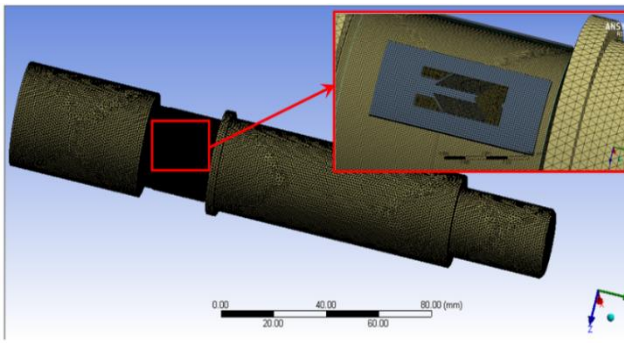

Fig.7 Elements and meshing shape

The gauge (grid) configuration scheme in the red area permitted the development of maximum sensitivity. The gauge configuration was also considered and analysed for four pieces, namely strain gauge 1, strain gauge 2, strain gauge 3, and strain gauge 4, and the linear variation in the alteration of the length with respect to the applied torque on the strain as shown in Figure 8 (a, b, c and d). The results are presented in Tables 3 to 6.

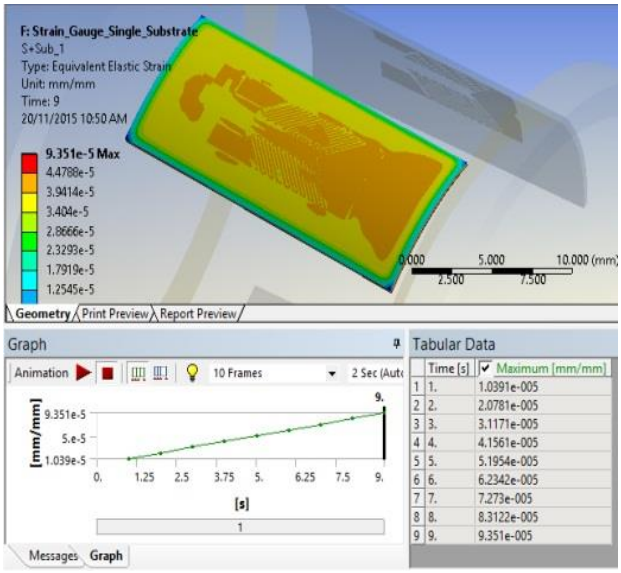

Fig. 8 .a Single strain gauge – 1

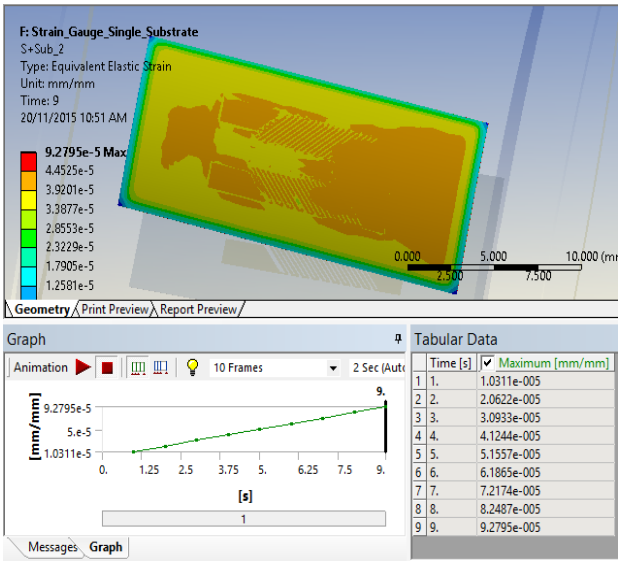

Fig. 8 .b Single strain gauge – 2

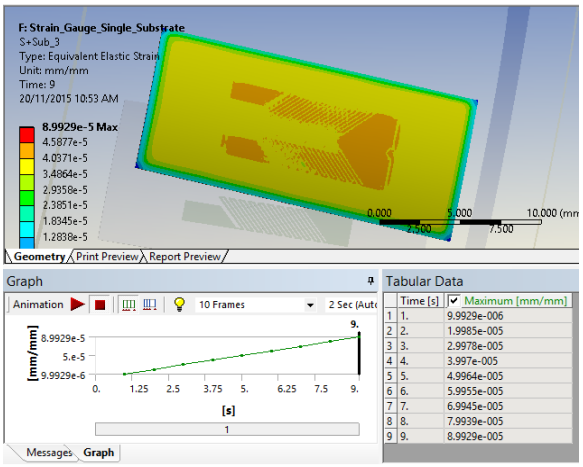

Fig. 8 .c Single strain gauge – 3

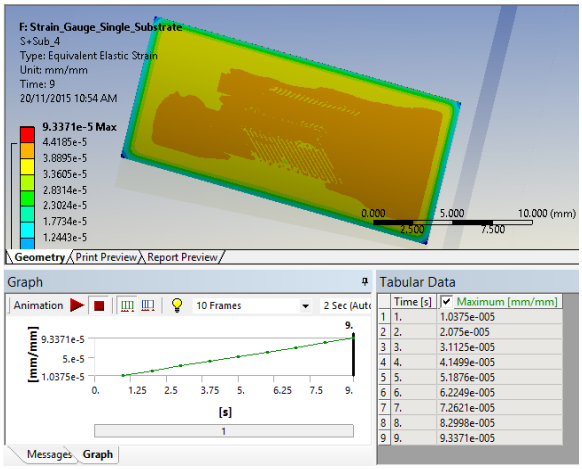

Fig. 8 .d Single strain gauge – 4

Table 3 Strain in substrates

Case	Mass (kg)	Torque (Nm)	Strain (%) Substrate 1	Strain (%) Substrate 2	Strain (%) Substrate 3	Strain (%) Substrate 4
1	0.00	0.0000	0.0000	0.0000	0.0000	0.0000
2	0.50	2.4525	1.0391E-05	1.0311E-05	9.9930E-06	1.0375E-05
3	1.00	4.9050	2.0781E-05	2.0622E-05	1.9985E-05	2.0750E-05
4	1.50	7.3575	3.1171E-05	3.0933E-05	2.9978E-05	3.1125E-05
5	2.00	9.8100	4.1561E-05	4.1244E-05	3.9970E-05	4.1499E-05
6	2.50	12.2625	5.1954E-05	5.1557E-05	4.9964E-05	5.1876E-05
7	3.00	14.7150	6.2342E-05	6.1865E-05	5.9955E-05	6.2249E-05
8	3.50	17.1675	7.2730E-05	7.2174E-05	6.9945E-05	7.2621E-05
9	4.00	19.6200	8.3122E-05	8.2487E-05	7.9939E-05	8.2998E-05
10	4.50	22.0725	9.3510E-05	9.2795E-05	8.9929E-05	9.3371E-05

Table 4 single strain gauge – Full Bridge

Case	Torque (Nm)	First strain Gauge (%)	Second strain gauge (%)	Third strain gauge (%)	Fourth strain gauge (%)
1	0.0000	0.0000	0.0000	0.0000	0.0000
2	2.4525	7.8260E-06	7.9630E-06	7.9350E-06	7.8790E-06
3	4.9050	1.5652E-05	1.5926E-05	1.5871E-05	1.5759E-05
4	7.3575	2.3478E-05	2.3889E-05	2.3806E-05	2.3638E-05
5	9.8100	3.1303E-05	3.1853E-05	3.1741E-05	3.1518E-05
6	12.2625	3.9131E-05	3.9817E-05	3.9678E-05	3.9399E-05
7	14.7150	4.6955E-05	4.7779E-05	4.7612E-05	4.7277E-05
8	17.1675	5.4779E-05	5.5740E-05	5.5546E-05	5.5154E-05
9	19.6200	6.2607E-05	6.3705E-05	6.3483E-05	6.3036E-05

The linear deviation of strain variation relating to the applied torque on the gauges is shown in Figure 9. This shows that the resistance of the gauge had a linear reaction to the applied torque. Moreover, the maximum applied torque and its conforming strain achieved for the aluminium substrate were 22.0725 Nm and 369.605 με, respectively. The non-linear performance of the substrate material improved after the torque was applied. These values were achieved by using the ANSYS simulation.

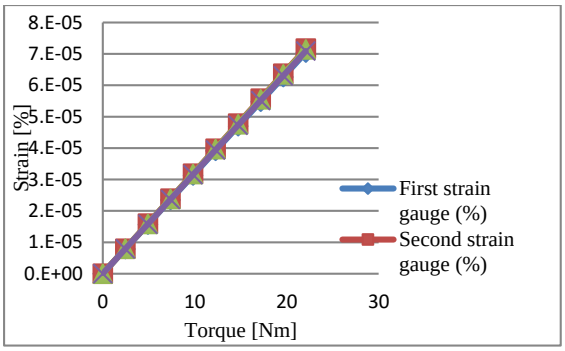

Fig. 1 the strains on the gauges when torque is applied

Table 5 Comparison between "strain gauge combine with substrate" together

Case	Torque (Nm)	Strain (%) Strain Gauge 1	Strain (%) Strain Gauge 2	Strain (%) Strain Gauge 3	Strain (%) Strain Gauge 4
1	0.0000	0.0000	0.0000	0.0000	0.0000
2	2.4525	2.7452E-05	2.7509E-05	2.7163E-05	2.7489E-05
3	4.9050	5.4902E-05	5.5017E-05	5.4325E-05	5.4978E-05
4	7.3575	8.2353E-05	8.2526E-05	8.1488E-05	8.2467E-05
5	9.8100	1.0980E-04	1.1004E-04	1.0865E-04	1.0996E-04
6	12.2625	1.3726E-04	1.3755E-04	1.3582E-04	1.3745E-04
7	14.7150	1.6471E-04	1.6505E-04	1.6298E-04	1.6493E-04
8	17.1675	1.9215E-04	1.9255E-04	1.9013E-04	1.9242E-04
9	19.6200	2.1961E-04	2.2007E-04	2.1730E-04	2.1991E-04
10	22.0725	2.4705E-04	2.4757E-04	2.4446E-04	2.4739E-04

Table 6 Compare between "strain gauge combine with substrate and shaft" together

Case	Torque (Nm)	Strain (%) Strain Gauge 1	Strain (%) Strain Gauge 2	Strain (%) Strain Gauge 3	Strain (%) Strain Gauge 4
1	0.0000	0.0000	0.0000	0.0000	0.0000
2	2.4525	2.7452E-05	2.7509E-05	2.7163E-05	2.7489E-05
3	4.9050	5.4902E-05	5.5017E-05	5.4325E-05	5.4978E-05
4	7.3575	8.2353E-05	8.2526E-05	8.1488E-05	8.2467E-05
5	9.8100	1.0980E-04	1.1004E-04	1.0865E-04	1.0996E-04
6	12.2625	1.3726E-04	1.3755E-04	1.3582E-04	1.3745E-04
7	14.7150	1.6471E-04	1.6505E-04	1.6298E-04	1.6493E-04
8	17.1675	1.9215E-04	1.9255E-04	1.9013E-04	1.9242E-04
9	19.6200	2.1961E-04	2.2007E-04	2.1730E-04	2.1991E-04
10	22.0725	2.4705E-04	2.4757E-04	2.4446E-04	2.4739E-04

In the tables above, it was noted that the output results for the four strain gauges were in truth almost four times the output values of the one strain gauge. What is more, in the case of the two strain gauges, the values were approximately twice the output values of the one strain gauge that was recycled in this research.

The values of the resistance changes of the four strain gauges of 350 Ω were actually identical. As a result, the basis of the new proposal was correlated to the value of each single strain gauge output that would be twice the output value of the theoretical as shown in Table 7

Table 7 the comparison between theoretical and simulation outputs

Method		Strain (%)	Vo/Vin (mV/V)	ΔR (Ω)
Theoretical		3.1820E-05	0.114552	0.0401
Simulation	Strain Gauge 1	7.0431E-05	0.253552	0.0887
	Strain Gauge 2	7.1667E-05	0.258001	0.0903
	Strain Gauge 3	7.1417E-05	0.257101	0.0899
	Strain Gauge 4	7.0913E-05	0.255287	0.0894

5 Torque Sensor

The CATIA software and ANSYS were used to design and analyse the torque sensor. This sensor consisted of a solid shaft, a substrate, and a gauge. A shaft, with a diameter of 28 mm, and with a maximum strain value, was selected for this study. Meanwhile, the minimum strain was found on the large diameter of the shaft. Therefore, the strain gauge was attached at the maximum strain range to accomplish maximum sensitivity. The strains on the sensor elements, for example, the shaft, the substrate, and the gauge, are shown in Figure 6. The strain established on the torque sensor and its apparatus is specified in Tables 8 and 9. It was used to calculate the ratio of the change in strain from one element to another element such as the shaft, substrate and gauge (grid), and assisted in the study into the sensible performance under changed weights, although this study permitted the selection of exact materials for the measurement and positioning of the modules before manufacture

Table 8 Strain transferred from substrate to Gauge

Case	Torque (Nm)	First strain gauge (%)	Second strain gauge (%)	Third strain gauge (%)	Fourth strain gauge (%)
1	0.0000	0.0000	0.0000	0.0000	0.0000
2	2.4525	75.31518	77.22820	79.40558	75.94217
3	4.9050	75.31880	77.22820	79.41456	75.94699
4	7.3575	75.32001	77.22820	79.41157	75.94538
5	9.8100	75.31821	77.23063	79.41206	75.94882
6	12.2625	75.31855	77.22909	79.41318	75.94842
7	14.7150	75.31840	77.23107	79.41289	75.94821
8	17.1675	75.31830	77.23003	79.41383	75.94773
9	19.6200	75.31941	77.23035	79.41430	75.94882
10	22.0725	75.31922	77.23153	79.41487	75.94756

Table 9 Strain transferred from Shaft to Substrate

Case	Torque (Nm)	First strain gauge (%)	Second strain gauge (%)	Third strain gauge (%)	Fourth strain gauge (%)
1	0.0000	0.0000	0.0000	0.0000	0.0000
2	2.4525	136.11001	137.16604	141.53098	136.31991
3	4.9050	136.11656	137.16604	141.53806	136.31991
4	7.3575	136.11874	137.16604	141.53570	136.31991
5	9.8100	136.11983	137.16604	141.53806	136.32320
6	12.2625	136.11263	137.16072	141.53381	136.31728
7	14.7150	136.11874	137.16826	141.53806	136.32210
8	17.1675	136.12311	137.17175	141.54312	136.32742
9	19.6200	136.11983	137.16771	141.53983	136.32320
10	22.0725	136.12311	137.17196	141.54357	136.32575

Strain gauges and their elements strain values for different rates of torque are set in Tables above. The ratio of the change in strain from one element to another element such as the shaft, substrate and gauge is constant for all torque.

That means the strain gauge arrangement is designed accurately on the greatest strained area of the substrate. This accomplishes the maximum sensitivity.

6 Conclusion

Computer system users, administrators, and designers usually have an objective of peak performance at lowest cost. A simulation is the execution of a model, represented by a computer program that gives information about the system being investigated. In this paper, strain gauge measurements involve two expert fields, namely electrical engineering and mechanical engineering. In a number of resource checks, it is especially crucial to understand the stress, which frequently comes about in the materials. The idea will lead to a significant conclusion concerning the structural balance of a material, regardless of its preceding shape and size. The objectives of this paper were achieved through practical experience with resistance strain measurement procedures and an understanding of the actual Wheatstone connection, as well as just how it is utilised in strain measurements. Research was conducted into the layout as well as the simulation of a piezoresistive material, as well as the torque sensor. The material that was purchased came with equations for determining the torsional base of the torque sensor. Aluminium was selected as an alternative substrate material for determining the desired strain. The most stretched places in the substrate were determined with regard to different border problems. The determined pattern was designed as well as analysed. The most stretched area and its equivalent pattern were picked for the determination of the strain. A torque sensor was designed using the actual design of the piezoresistive material with its determined strain, and the simulation results indicated that the resistance change was usually linear towards the utilized torque. The results of the simulation enabled the percentage of strain transported in the base from the shaft to the substrate and then to the gauge to be calculated. The actual purpose of this was to calculate the precise strain percentages of the sensor parts. At the end, the simulation approach of analysing a model is opposed to the analytical approach, where the method of analysing the system is purely theoretical. As this approach is more reliable, the simulation approach gives more flexibility and convenience. A proper knowledge of both the techniques of simulation modeling and the simulated systems themselves are needed to achieve the new design.

Acknowledgment

This work was supported by the Mechanical & Materials Engineering Department, Faculty of Engineering & Built Environment of Universiti Kebangsaan Malaysia 43600 UKM Bangi, Malaysia, Department of Mechanical Engineering, College of Engineering, Universiti Tenaga Nasional, Putrajaya Campus, Jalan Ikram-Uniten, 43000 Kajang, Selangor, Malaysia, the Computer Science Department, Faculty of Science, Libyan Sirte University, Sirte, Libya and the Department of Agra-energetics and foods Engineering, Faculty of Mechanical Engineering, Szent Istvan University, H 2103, Godollo, Hungary. They are gratefully acknowledged.

Conflict of interest: The authors declare that there are no conflicts of interest.

References

Cao, L., Kim, T. S., Mantell, S. C. & Polla, D. L. 2000. Simulation and Fabrication of Piezoresistive Membrane Type Mems Strain Sensors. *Sensors and Actuators A: Physical* 80(3): 273-279.

Eaton, W. P., Bitsie, F., Smith, J. H. & Plummer, D. W. 1999. A New Analytical Solution for Diaphragm Deflection and Its Application to a Surface Micromachined Pressure Sensor. *International Conference on Modeling and Simulation, MSM*, hlm.

Eberlein, D. 2008. Applying the Wheatstone Bridge Circuit. www.hbm.com [20 September 2015].

Hamid, M. Y., Thangamani, U. & Vaya, P. R. 2006. Simulation of Piezo-Resistive Metal Gauge on Rectangular Membrane for Low Pressure Application. *Semiconductor Electronics, 2006. ICSE '06. IEEE International Conference on*, hlm. 304-308.

Hoffmann, K. 1989. *An Introduction to Measurements Using Strain Gages*. Germany: Hottinger Baldwin Messtechnik GmbH.

J.W.Dally & W.F.Riley. 1991. *Experimental Stress Analysis*. 3. New York: McGraw-Hill.

Joyce, D. & Scott, M. 1993. Force and Mass Determination by Strain Gauge. *Significance of Calibration, IEE Colloquium on*, hlm. 3/1-310.

Korzenszky, P. 2009. Grinding Kinetic and Energetic Examination of Hammer Mills. Tesis PhD, Faculty of Mechanical Engineering, St. István University, Gödöllő, Hungary.

Wang Y.J., Zuo G.K., Chen X.L., Liu L. Strain analysis of six-axis force/torque sensors based on analytical method. *IEEE Sens. J.* 2017;**17**:4394–4404. doi: 10.1109/JSEN.2017.2703160.

Hu G.Y., Gao Q., Cao H.B., Pan H.Q., Shuang F. Decoupling analysis of a six-dimensional force sensor bridge fault. *IEEEAccess.* 2018;**6**:7029–7036. doi: 10.1109/ACCESS.2017.2784485.

Li X., He H., Ma H.Q. Structure design of six-component strain-gauge-based transducer for minimum cross-interference via hybrid optimization methods. *Struct. Multidiscip.Optim.* 2019;**60**:301–314. doi: 10.1007/s00158-018-2177-y.

A Lever-Type Method of Strain Exposure for DiskF-Shaped Torque Sensor DesignRan Shu, Zhigang Chu and Hongyu Shu, *1State Key Laboratory of Mechanical Transmissions, Chongqing University, Chongqing 400044, (R.S.); (Z.C.)2College of Automotive Engineering, Chongqing University, Chongqing 400044; Published: 19 January 2020

Lin, L., Chu, H.-C. & Lu, Y.-W. 1999. A Simulation Program for the Sensitivity and Linearity of Piezoresistive Pressure Sensors. *Microelectromechanical Systems, Journal of* 8(4): 514-522.

Micro-Measurements, V. 2007. Optimizing Strain Gage Excitation Levels. *Tech Note TN* 502(15).

Murray, W. M. & Miller, W. R. 1992. *The Bonded Electrical Resistance Strain Gage*. Oxford University Press.

Orhan, M. H., Dogan, C., Kocabas, H. & Tepehan, G. 2001. Experimental Strain Analysis of the High Pressure Strain Gauge Pressure Transducer and Verification by Using a Finite Element Method. *Measurement Science and Technology* 12(3): 335.

Schomburg, W., Rummler, Z., Shao, P., Wulff, K. & Xie, L. 2004. The Design of Metal Strain Gauges on Diaphragms. *Journal of Micromechanics and Microengineering* 14(7): 1101.

Szilard, R. 1974. Theory and Analysis of Plates.

Thangamani, U., Mohd Yunus, H. & Ali, C. 2008. Design and Simulation of Force Sensor with Piezo Resistive Rectangular Strain Gauge.

Window, A. L. & Holister, G. S. 1982. *Strain Gauge Technology*. Applied science publishers.

Yang, S. & Lu, N. 2013. Gauge Factor and Stretchability of Silicon-on-Polymer Strain Gauges. *Sensors* 13(7): 8577-8594.

Young, W. C. & Budynas, R. G. 2002. *Roark's Formulas for Stress and Strain*. McGraw-Hill New York.

Ahmet Kara / Procedia - Social and Behavioral Sciences 237 (2017) 882 – 886, Simulations of information technology-induced teaching performance in cross-disciplinary settings: a model and an application, Published by Elsevier Ltd. *7th International Conference on Intercultural Education "Education, Health and ICT for a Transcultural World", EDUHEM 2016, 15-17 June 2016, Almeria, Spain*

Scientific Journal for faculty of Science
Sirte University

sjsfsu@su.edu.ly
journal.su.edu.ly/index.php/JSFSU

media92production@gmail.com
قسم الإنتاج الإعلامي جامعة سرت
تصميم : عبدالله نصرالدين